HYBRID LES MONTE-CARLO PDF MODELING OF TURBULENT PILOTED JET FLAMES

Jens Kuehne, Clemens Olbricht, Amsini Sadiki, Johannes Janicka
Institute for Energy and Powerplant Technology,
Darmstadt University of Technology
Petersenstr. 30, D-64287 Darmstadt, Germany
kuehne@ekt.tu-darmstadt.de

Jyh-Yuan Chen
Combustion Modeling Laboratory,
University of California at Berkeley
6163 Etcheverry Hall, Berkeley, CA 94720, USA

ABSTRACT

The development of an adaptive particle redistribution method for Eulerian Monte-Carlo simulation of joint scalar probability density function coupled with LES is described. The proposed method is assessed with two test cases, namely the Sandia/TUD turbulent piloted methane/air jet flames D and F. Numerical results of the transported mixture fraction and its fluctuations are compared on the one hand side to a calculation with an uniformly distributed amount of particles and on the other hand side with experimental data.

INTRODUCTION

Better knowledge of mixing and combustion dynamics in turbulent flows becomes cumulatively important, especially to achieve high efficiency and low emission in modern gas turbines. In this regard CFD has become an important tool of optimization processes pollutant emissions and reduction of development phases of novel constructions. However, accurate prediction of flow, mixing and combustion processes and dynamics require a comprehensive set of numerical submodels, since direct numerical simulation (DNS) is too expensive [Janicka and Sadiki (2005)].

A promising tool for reliable predictions of unsteady phenomena as occurring in turbulent reacting flows is the large eddy simulation (LES). LES can be seen as a compromise between Reynolds averaged Navier Stokes (RANS) and DNS, computing the large scale structures while modeling the small scale influence of the turbulence. Nevertheless, the information on the small scales are necessary for their influence on the turbulence-chemistry interaction and especially on the chemical reaction rates. These rates show a highly non-linear behavior with the crucial properties in the modelling.

With respect to this, it is essential to be aware of the joint probability density function (JPDF) of the transported scalar within the subgrid. Commonly, the so called presumed β-PDF approach is used [Rhodes (1975)]. Here, scalar PDF's are standardized in terms of scalar means and variances. In combustion processes characterized by several involved species the assumed PDF method needs further assumptions and is computational expensive [Pope (1994)]. Furthermore the presumed shape of the subgrid PDF is a restrictive approximation in cases of complex mixing and high turbulence-chemistry interaction. Olbricht et al. (2006) showed, that the presumed β-PDF's have a strong smoothing character and that often occurring complex micromixing situations cannot be well described by this PDF.

In order to avoid this lack a modelled transport equation for the composition PDF is solved. In general, this equation is highly dimensional and thus impractical to be solve using a finite volume method. Hence, the Monte-Carlo method has been used to solve this PDF transport equation in which the PDF is represented by an ensemble of stochastic particles. One major advantage of the transported PDF method is that the filtered chemical reaction source term appears in closed form and thus has not to be modelled.

In the present paper the hybrid LES Monte-Carlo PDF approach is extended by an adaptive method. Within the following chapters this method is described in detail. For proving of the accuracy of the method along with its numerical implementation two configurations are considered, Sandia/TUD flame D and F, which are turbulent piloted methane/air jet flames experimentally investigated by Barlow and Frank (1998) and Schneider et al. (2003).

GOVERNING EQUATIONS

In reactive cases like combustion the density changes in time as a function of temperature and concentration. Following the spatial filtering procedure made to obtain the filtered equations for LES the appearance of unclosed terms according to these density changes can be avoided by using Favre-filtering (density-weighted filtering: $\bar{\rho}\widetilde{\phi} = \overline{\rho\phi}$). Equations (1) and (2) represent the Favre-filtered conservation of mass and momentum for fluids with Newtonian behavior.

$$\frac{\partial \bar{\rho}}{\partial t} + \frac{\partial}{\partial x_j}(\bar{\rho}\widetilde{u}_j) = 0 \tag{1}$$

$$\begin{aligned}\frac{\partial}{\partial t}(\bar{\rho}\widetilde{u}_i) + \frac{\partial}{\partial x_j}(\bar{\rho}\widetilde{u}_i\widetilde{u}_j) = \\ \frac{\partial}{\partial x_j}\Big(\bar{\rho}\widetilde{\nu}\Big(\frac{\partial \widetilde{u}_i}{\partial x_j} + \frac{\partial \widetilde{u}_j}{\partial x_i}\Big) \\ -\frac{2}{3}\bar{\rho}\widetilde{\nu}\frac{\partial \widetilde{u}_k}{\partial x_k}\delta_{ij} + \bar{\rho}\tau_{ij}^{sgs}\Big) - \frac{\partial \bar{p}}{\partial x_i}\end{aligned} \tag{2}$$

Thereby the unresolved term τ_{ij}^{sgs} are due to the nonlinearity of the convective term. This so called subgrid scale stress tensor is closed by the standard Smagorinsky model [Smagorinsky (1963)].

$$\tau_{ij}^{sgs} - \frac{1}{3}\tau_{kk}^{sgs}\delta_{ij} = 2\nu_t \widetilde{S}_{ij} \quad \text{with} \quad \nu_t = (C_S\bar{\Delta})^2|\widetilde{S}_{ij}| \quad (3)$$

$$\widetilde{S}_{ij} = \frac{1}{2}\Big(\frac{\partial\widetilde{u_i}}{\partial x_j} + \frac{\partial\widetilde{u_j}}{\partial u_i}\Big) \quad (4)$$

The model coefficient C_S is dynamically calculated by the procedure originally proposed by Germano et al. (1991) with the modifications suggested by Lilly (1992). $\bar{\Delta}$ in equation (3) represents the averaged filter width, which coincides with the size of the grid cells.

In Pope (1981) it is shown, that the development of the scalar PDF $P(\psi; x, t)$ can be described by a multidimensional transport equation. This PDF evolves in physical space (x, t) as well as in composition space $\psi(= \psi_1, \psi_2, ...)$, which determines the stochastic variables for the scalars $\phi(= \phi_1, \phi_2, ...)$. The transport equation for the Favre-filtered PDF reads as follows:

$$\frac{\partial}{\partial t}(\bar{\rho}\widetilde{P}) + \frac{\partial}{\partial x_i}(\bar{\rho}\widetilde{P}\widetilde{u_i}) + \frac{\partial}{\partial \psi_\alpha}(\bar{\rho}\widetilde{P}S_\alpha) = \quad (5)$$

$$\frac{\partial}{\partial x_i}\Big[\bar{\rho}(\widetilde{D} + D_t)\frac{\partial\widetilde{P}}{\partial x_i}\Big] + E(\psi; x, t) \quad (6)$$

Here, the left hand side includes the accumulation, the convection and the chemical source terms. The first term on the right hand side represents the diffusive transport in physical space which is followed by the molecular mixing term in composition space. The terms on the left hand side of equation (6) including the chemical source term exist in a closed form, whereas the terms on the right hand side have to be modelled. Thereby the turbulent diffusion has been approximated by a gradient assumption.

Since the PDF's are commonly multidimensional with a variety of transported scalars, one has to take care of the efficiency of the used solver for equation (6) in order to keep the computational effort as low as possible. The Monte-Carlo method requires a computational effort which is rising linearly with the number of transported scalars and thus is the best choice for solving the PDF transport equation. For comparison, the computational effort of a finite difference scheme increases exponentially with the number of unknown variables [Pope (1981)].

NUMERICAL PROCEDURE

In the context of this work the three dimensional CFD code FLOWSI is used. For transported PDF calculations a stochastic Eulerian Monte-Carlo solver was integrated in framework of the existing finite-volume LES code. The code is based on an axis symmetric staggered grid. The time integration uses an explicit three-step low-storage Runge-Kutta scheme. The momentum transport is second order in space, while the finite-volume transport for the scalars is carried out with a predictor/corrector approach using TVD-schemes [Kempf (2003)] and hence reaching second order accuracy away from sharp gradients.

The Monte Carlo method uses an ensemble of stochastic particles to represent the PDF's. The present paper handles the Eulerian approach of the Monte Carlo method in which the ensemble of stochastic particles are fixed in physical space in contrast to the Lagrangian approach, where the particles follow the flow. In order to solve the PDF transport equation the Fractional Steps method proposed by Pope (1985) is applied. Here, the actual simultaneous proceeding effects, convection, diffusion, chemistry and mixing are processed in sequence as shown in equation (7).

$$\widetilde{P}(\psi; t + \Delta t) = (I + \Delta t\mathcal{C})(I + \Delta t\mathcal{M})(I + \Delta t\mathcal{R})\widetilde{P}(\psi; t) \quad (7)$$

The approximation of the PDF $\widetilde{P}(\psi; t + \Delta t)$ by using the Fractional Steps method implies an error of order Δt. The three fractional steps are namely the convective and diffusive transport $\mathcal{C}$, the mixing process $\mathcal{M}$ and the chemical reaction $\mathcal{R}$. The applied models for the three processes are described below.

The convective and diffusive transport is approximated by upwind discretization. The simulation of this transport is accomplished by an exchange of values of the stochastic particles between adjacent cells.

The molecular mixing process is modelled by the so called Modified Curl's model [Janicka et al. (1979)], which is based on a pairwise interaction between stochastic particles. The effect of using different sgs-mixing models in LES context is investigated by Bisetti and Chen (2005).

In the present paper the chemical process $\mathcal{R}$ is neglected, since the transported scalar mixture fraction is commonly a non-reacting property without any sources. This is the case as long as there is no phenomenon related to two phase flows with phase changes. Nevertheless, flamelet tables created by the chemical kinetics tool CHEM1d [Hermanns (2001)] are used to determine the thermodynamic and chemical state. Therefor, the tables are entered with the calculated mixture fraction value of each particle and returns information about density, temperature and several chemical species. By using Monte Carlo PDF methods it turns out that it is not required to make a β-integration of the flamelet table over the variance of the mixture fraction. In comparison to a pre-integrated flamelet table the memory usage is lower, since the tables have less dimensions.

ADAPTIVE PARTICLE DISTRIBUTION METHOD

The adaptive method aims at an effective usage of the implemented Monte Carlo PDF method. The idea is to redistribute the actually fixed stochastic particles in a way that there is a higher density of particles in areas of interest, for example the reaction zone. With such an approach the statistical error can be reduced with the same memory consumption and nearly the same computational effort. The new distribution of the particles can be calculated by an arbitrary function. The present work introduces and investigates a distribution function which is based on two major assumptions:

- The PDF of a well mixed scalar field can be uniquely defined by a single stochastic particle
- The standard error ϵ_N depends linearly on the variance of the scalar

From the first assumption it appears, that a DNS calculation needs only as many particles as cells. The DNS cell size should be chosen according to Kolmogorov's scale η, which is the smallest scale of turbulence. That implies, that inside this microscales all fields are well mixed and hence the PDF can be represented by a single particle. Kolmogorov's approach of comparing the integral length scale L with Kolmogorov's scale is known as

$$\frac{L}{\eta} = \mathrm{Re}^{3/4} \quad (8)$$

This equation is used to make an estimation of the maximum number of particles, which is needed for an exact representation of the PDF in a given LES cell. For application in a three dimensional problem equation (8) has to be taken to the third power. Substitution of the integral length scale L with the LES cell width Δ_{LES} leads to equation (9).

$$\left(\frac{L}{\eta}\right)^3 = \frac{\Delta_{LES}^3}{\Delta_{DNS}^3} = (\mathrm{Re}^{3/4})^3 = \mathrm{Re}^{9/4} \tag{9}$$

Taking the first assumption into account and inserting it in equation (9) one gets the correlation of the ideal particle amount for the LES cell size:

$$\frac{N_{LES}^{max}}{N_{DNS}^{max}} = \frac{N_{LES}^{max}}{1} = \mathrm{Re}^{9/4} \tag{10}$$

The present work uses a local turbulent Reynolds number to calculate equation (10), which is defined by

$$\mathrm{Re}_t = \frac{u^{`}\bar{\Delta}}{\nu_t} \tag{11}$$

Here, $u^{`}$ denotes the velocity fluctuations, $\nu_t$ the turbulent viscosity and $\bar{\Delta}$ the average cell length. The velocity fluctuations are not entirely resolved and so a model for the spatial unresolved part of $u^{`}$ has to be used. This work makes use of the model proposed by Yoshizawa (1982) for the unresolved turbulent kinetic energy k_{sgs}.

$$k^{total} = k^{resolved} + k^{sgs} = k^{resolved} + (\frac{1}{(C_v\bar{\Delta})^2}\nu_t^2) \tag{12}$$

The constant C_v is defined according to Scotti et al. (1993) as $C_v = 0.1$. Eventually the ideal particle density for each cell can be computed by using equation (13).

$$N_{LES}^{max} = \mathrm{Re}_t^{\frac{9}{4}} = \left(\frac{\sqrt{\frac{2}{3}(k^{resolved} + \frac{1}{(C_v\bar{\Delta})^2}\nu_t^2)}\bar{\Delta}}{\nu_t}\right)^{\frac{9}{4}} \tag{13}$$

The second assumption is, that the standard error is linearly proportional to the variance of the mixture fraction and inversely proportional to the square root of the number of particles inside the ensemble [Pope (1985)].

$$\epsilon_N = \frac{\sigma}{\sqrt{N}} \tag{14}$$

From equation (14) by approaching a constant standard error, one can derive a relation between the particle density N and the sgs-variance.

$$N \sim \sigma^2 = \langle f^{`2}\rangle \tag{15}$$

$\sigma = \langle f^{`2}\rangle^{\frac{1}{2}}$ denotes the second central moment of the mixture fraction f. In this work, the normalized variance, the so called unmixedness ξ is inserted into equation (15). The unmixedness is normalized by the maximum value of the variance $f(1-f)$. Hence, one obtains equation (16).

$$N \sim \frac{\langle f^{`2}\rangle}{f(1-f)} = \xi \tag{16}$$

Taking both relations (13) and (16) into account one obtains the eventual relation between the particle density, the flow characteristics and the mixing properties.

$$N = N_{LES}^{max} \cdot \xi \tag{17}$$

Obviously, the distribution function of N must be reasonably continuous in time in order to keep the error due to the change of the particle density as low as possible. Unfortunately the local turbulent Reynolds number Re_t and accordingly N_{LES}^{max} vary in time, because the turbulent viscosity ν_t is not continuous in time due to the used eddy-viscosity model. Thus, we use a time averaged $\overline{N}_{LES}^{max}$ as a matrix and include the time dependence of the particle density by the unmixedness $\xi(t)$ [see equation (18)].

$$N(t) = \overline{N}_{LES}^{max} \cdot \xi(t) \tag{18}$$

Kuehne (2006) compared different adaptation frequencies and concluded to prefer a frequency of twenty time steps. The procedure of adaptation is described below. At first, the new number of particles for each cell is calculated according to the distribution function. Dependent on the relation between the previous and the newly calculated amount of particles per cell different procedures are possible [Permana and Chen (2003)].

1. previous and new number of particles are the same: all values of the particle ensemble are copied
2. previous amount of particles in a cell is larger than the new one: the values of the new ensemble are randomly chosen out of the existing one
3. previous particle density is lower than the new one: the values of the existing particles are copied as often as the integer of the ratio new to previous amount, the values of the remaining particles are again chosen randomly from the previous ensemble

It is evident, that the calculated distribution of the particles does not result in the same total amount of particles as the simulation is initialized. Hence, the adaptation procedure distributes the particles according to the given function as long as the total number of particles is reached. Concisely, the total number of particles in the domain is kept constant and there is a redistribution of the given particle ensemble.

CONFIGURATION

The investigated configuration in this contribution is a non-premixed piloted methane/air jet flame measured at the Sandia National Laboratory and the Darmstadt University of Technology [Barlow and Frank (1998)]. The center nozzle has a diameter of $D_{jet} = 7.2mm$ and the pilot flame has a diameter of $D_{pilot} = 18.2mm$. The fuel consists of 25% of methane CH_4 and 75% of air. The stoichiometric mixture fraction is $f_{st} = 0.351$. The fuel of the pilot flame is a premixed composition of acetylene C_2H_2, hydrogene H_2, air, carbon ioxode CO_2 and nitrogen N_2. Experiments show, the flames behave like non-premixed flames, even though a premixed composition is inserted from the center nozzle. Around the pilot flame a so called coflow with a low speed air flow is arranged, in order to protect the flame from extrinsic interferences. Different Reynolds numbers have been applied to this configuration and build a series of flames, which are called Sandia/TUD flame A, B, C, D, E and F. In this work flame D and F with the properties shown in table 1 are investigated.

The computational domain for the simulations has a length of 20 jet diameters in axial direction and 10 jet diameters in the radial direction. The domain is discretized by grids with 280000 cells (flame D) and 960000 cells (flame F), respectively. The uniform particle distribution at initialization is 20 particles per cell for both flames and hence

Table 1: Properties of the Sandia/TUD flames D and F

	$U_{jet}[\frac{m}{s}]$	$U_{pilot}[\frac{m}{s}]$	$U_{co}[\frac{m}{s}]$	$Re_{jet}[-]$
Flame D	49.6	11.4	0.9	22400
Flame F	99.2	22.8	0.9	44800

gives total numbers of particles of $N_{tot}^{D} = 5.6 \cdot 10^6$ and $N_{tot}^{F} = 19.2 \cdot 10^6$ for flame D and flame F, respectively.

RESULTS

Figure 1 shows the distributions of the ideal particle density $\overline{N}_{LES}^{max}$ averaged .for the two investigated cases flame D and F. As one can clearly see, the structures of the more turbulent flame F on the right hand side are smaller than the ones of flame D. Furthermore flame F shows higher values for this property in general. As one would expect, $\overline{N}_{LES}^{max}$ is higher near the inlet boundary, which is caused by larger velocity fluctuations according to the existence of two mixing layers. On the one hand side between the main jet and the surrounding pilot and on the other hand side between the pilot and the coflow. The highest values range around 90000 particles per cell whereas the lowest numbers are approximately 300.

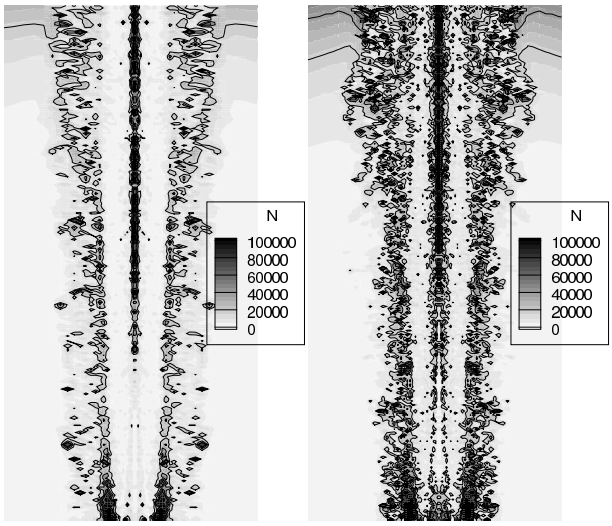

Figure 1: Distribution of the ideal particle density $\overline{N}_{LES}^{max}$ averaged over 5000 time steps. Flame D on the left and flame F on the right.

Figure 2 depicts instantaneous captures of the particle density $N(t)$ for flame D and F. The mixing layers contain the highest amounts of particles, this can easily be seen in the inlet region, where two mixing layers are present. Inside the flame, near the centerline, one can observe a low particle density which is associated to the absence of any mixing phenomena. The comparison of both configurations does not show any outstanding differences within the particle distributions except for the higher number of particles in flame F caused by a finer grid. The highest level of the particle density is around 45 for flame D and 60 for flame F.

Looking at the quantitative results in figure 3 one can see radial distributions of the mixture fraction (left) and its standard deviation (right) for flame D. The results are shown for three different axial positions, namely x/d =2, 7.5 and 15. The plots compare results of simulations using a constant particle density of 20 ppc with the above described

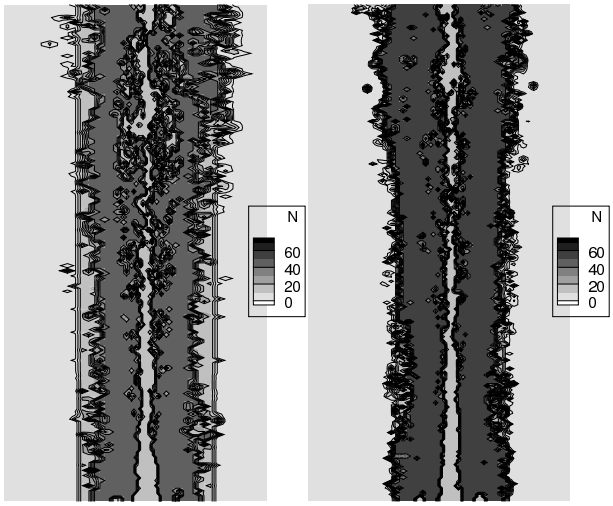

Figure 2: Instantaneous capture of the particle density. Flame D on the left and flame F on the right.

adaptive method and experimental data. Besides the mixture fraction results the average of the particle density is represented. At first it should be mentioned that the standard deviation plots are scaled in order to identify differences in the results more accurately.

The adaptive method shows consistently better results than the simulation with an uniformly distributed particle field in all axial positions. Nevertheless, the particle density near the inlet at x/d =2 is still too low, which is apparent at r/d =0.75 where the experimental data is still affected by the inlet boundary conditions. Both simulations do not show this behavior since the mixing of the pilot and the main jet seems to be too high. The fluctuations of the mixture fraction are as well dominated by the good results of the adaptive method. The adaptive method shows good agreement with the experiments especially at $x/d = 15$. Here, the uniform particle density calculation underpredicts the fluctuations at higher r/d ratios. Especially at x/d =2 the level of the fluctuations is too low. This is due to the fact, that the resolution of the grid within the inlet region is too coarse and thus the developing mixing layer cannot be calculated properly. This effect decreases by going downstream and so the level of the calculated fluctuations are similar to the experiments. A further aspect regarding the fluctuations is the underprediction near the centerline in all axial positions. This phenomenon is due to problems with the axis symmetric mesh. The cylindric grid arrangement implies that the transport over the centerline is challenging. Especially the Monte-Carlo procedure shows difficulties in the implementation, since a positive weighting scheme (e.g. upwind scheme) has to be used in order to realize the particle exchange between the cells. At this moment transport of particles over the centerline is not implemented and thus effects the fluctuation results near r/d =0. This might be confirmed by good results as soon as one moves from the centerline to the outer regions.

Figure 4 shows the same properties as figure 3 for flame F. This flame has significant and increasing probability of local extinction above the pilot region and is close to global extinction in the downstream part of the flame [Barlow and Frank (1998)]. Since the used chemistry table does not include extincted flamelets, it is obvious that the calculated results for flame Fdo not agree with the corresponding experiments. This is caused by severe density differences between burning and non-burning gas in reality which affect the flow

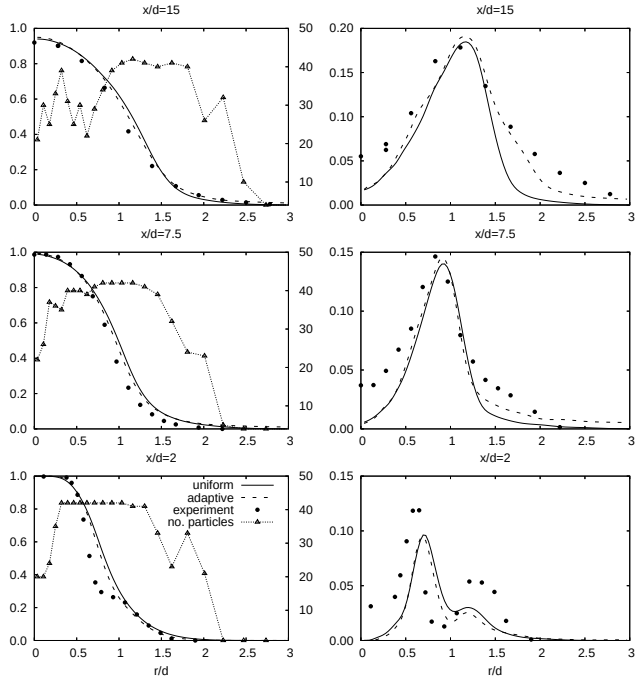

Figure 3: Radial distribution of the mixture fraction for three axial positions (left) and rms values of the mixture fraction (right) of flame D. Uniform particle density 20 ppc (solid lines), adaptive method(dashed lines), experimental data (symbols) [Barlow and Frank (1998)], particle density of adaptive method (dotted lines with triangles).

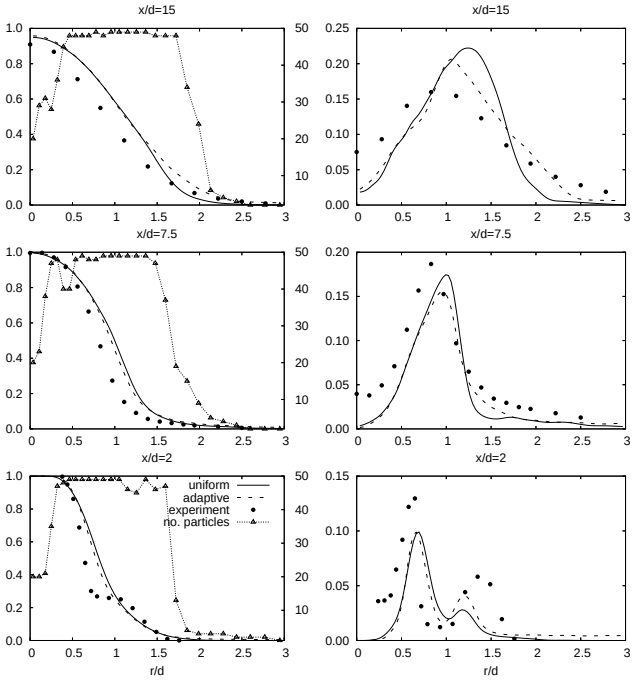

Figure 4: Radial distribution of the mixture fraction for three axial positions (left) and rms values of the mixture fraction (right) of flame F. Uniform particle density 20 ppc (solid lines), adaptive method(dashed lines), experimental data (symbols) [Barlow and Frank (1998)], particle density of adaptive method (dotted lines with triangles).

and the associated mixing significantly. The averaged mixture fraction results of the adaptive method as well as the calculation with uniform particle density show acceptable agreement with the experimental data for axial position x/d =2 with increasing discrepancy by moving further downstream. At position x/d =2 the same effect appears as in flame D. Apparently, there is a lack of both grid resolution and particle density, since the mixing between the pilot stream and the main jet is too high. This may also be caused by the high numerical diffusion due to the first order upwind scheme, which melts the influence of the inflow boundary conditions too fast. The calculations overpredict the mixture fraction values in almost all radial positions for x/d = 7.5 and 15. At x/d =15 the adaptive method does not really increase the accuracy of the simulation but even decreases it in the outer region. The depicted fluctuation plots show diverse behavior. The rms values near the inlet are too low due to the same reasons as described above in figure 3. At x/d =7.5 the adaptive method catches the experiments quite accurately at r/d higher than unity but underpredicts the peak compared to the uniform particle density calculation. Further downstream at x/d =15 the both calculations show fluctuations that are higher than the experimental results. Nevertheless the adaptive method gives better agreement than the simulation with uniform particle density.

CONCLUSION

An adaptive particle distribution method for a hybrid Eulerian Monte-Carlo PDF approach coupled with LES has been introduced and its applicability has been proven by simulations of the two turbulent piloted methane/air jet flames, Sandia/TUD flame D and F. Two simulations were carried out for each case, a calculation with uniform particle density in the domain and one with an adaptive particle distribution. The adaptive method aims at an increase of accuracy of the results by decreasing the statistical error within regions of interest in the flow. Therefor, a distribution function has been presented, which includes effects of the flow characteristics as well as mixing properties for the particle redistribution. The simulations with particle adaption show improvements of results for the time averaged mixture fraction and the fluctuations, respectively, for both investigated cases. Nevertheless the local extinctions of flame F could not be simulated since the used flamelet model is not able to represent extinction properly, yet. Concisely it can be said, that the goal of decreasing the statistical error due to a lack of particles is achieved. Furthermore the adaptive Monte-Carlo PDF calculations are a good choice for simulations of the jet flames investigated here according to the effective usage of the total amount of particles, because the statistical error can be controlled.

Future work will concentrate on the implementation of the adaptive method in a parallelized code version, which allows larger calculation domains and higher total amounts of particles at all. Another aspect will be to prove the applicability of this method in different configurations with complex geometries.

ACKNOWLEDGEMENT

For financial support we gratefully acknowledge the "German Research Foundation (DFG)".

REFERENCES

R.S. Barlow and J.H. Frank. Effects of Turbulence on Species

Mass Fractions in Methane-Air Jet Flames. *Proc. Comb. Inst.*, 27:1087–1095, 1998.

F. Bisetti and J.Y. Chen. LES of Sandia Flame D with Eulerian PDF and Finite-Rate Chemistry. 2005. Western State Section/Combustion Institute, 2005 Fall Meeting, Stanford.

M. Germano, U. Piomelli, P. Moin, and W.H. Cabot. A dynamic subgrid-scale eddy viscosity model. *Phys. Fluids A*, 3(7):1760–1765, 1991.

R.T.E Hermanns. CHEM1D, a one-dimensional laminar flame code. 2001. Report, Eindhoven University of Technology.

J. Janicka and A. Sadiki. Large eddy simulation of turbulent combustion systems. *Proc. Comb. Inst.*, 30:537–547, 2005.

J. Janicka, W. Kolbe, and W. Kollmann. Closure of the Transport Equation for the Probability Density Function of Turbulent Scalar Fields. *Journal of Non-Equilibrium Thermodynamics*, 4:47–66, 1979.

A. Kempf. *Large-Eddy Simulation of Non-Premixed Turbulent Flames*. PhD thesis, Darmstadt University of Technology, 2003.

J. Kuehne. LES of a Reacting Turbulent Jet Using an Adaptive Monte Carlo Method for PDF Modeling. Master's thesis, Darmstadt University of Technology / University of California, Berkeley, 2006.

D.K. Lilly. A proposed modification of the Germano subgrid-scale closure method. *Phys. Fluids A*, 4(3):633–635, 1992.

C. Olbricht, A. Sadiki, J. Janicka, and J.Y. Chen. Study of heat and mass transfer in complex mixing devices using a hybrid LES-Monte-Carlo PDF method. *International Conference of Heat and Mass Transfer, ICHMT 2006*, 2006.

A. Permana and J.Y. Chen. Adaptive Monte Carlo Method for PDF Modeling of Opposed Jet Reacting Flows. 2003. Western State Section/Combustion Institute, 2003 Fall Meeting, Los Angeles.

S.B. Pope. A Monte Carlo Method for the PDF Equations of Turbulent Reactive Flow. *Combustion Science and Technology*, 25:159–174, 1981.

S.B. Pope. PDF Methods for Turbulent Reactive Flows. *Progress in Energy and Combustion Science*, 11:119–192, 1985.

S.B. Pope. Lagrangian PDF methods for turbulent flows. *Annual Rev. Fluid Mech.*, 26:23–63, 1994.

R.P. Rhodes. A probability distribution function for turbulent flows. *Turbulent Mixing in Nonreacting and Reacting Flows*, 41:235–241, 1975.

Ch. Schneider, A. Dreizler, J. Janicka, and E.P. Hassel. Flow field measurements of stable and locally extinguishing hydrocarbon-fuelled jet flames. *Combust. Flame*, 135: 185–190, 2003.

A. Scotti, C. Meneveau, and D.K. Lilly. Generalized Smagorinsky model for anisotropic grids. *Physics of Fluids*, 5:2306–2308, 1993.

J. Smagorinsky. General circulation experiments with the primitive equations: I. the basic equations. *Mon. Weather Rev.*, 91:99–164, 1963.

A. Yoshizawa. A statistically-derived subgrid model for the large-eddy simulation of turbulence. *Physics of Fluids*, 25: 1532–1538, 1982.